Journal of Optoelectronics and Advanced Materials Vol. 5, No. 4, December 2003, p. 939 - 944

FIRST ORDER REVERSAL CURVES DIAGRAM FOR SOFT MAGNETIC MATERIALS

M. Fecioru-Morariu*, A. Stancu

„Al. I. Cuza“ University, Faculty of Physics, 11 Bd. Carol I, 6600 Iasi, Romania

Since the Jiles-Atherton model is often used to model magnetization curves in soft magnetic materials, we have simulated systematically First Order Reversal Curves (FORC) using this model and we have calculated the FORC diagrams to check the concordance between the experimental data and the model. We have studied the dependence of the FORC diagram as a function of the shape of pinning parameter and as a function of the model parameters: the value of pinning parameter (k) and the mean field parameter (α).

(Received July 4, 2003; accepted August 21, 2003)

Keywords: FORC diagrams, Jiles-Atherton model, Soft magnetic materials

1. Introduction

One of the recent methods for the magnetic characterization of magnetic materials is the First Order Reversal Curves (FORC) diagram, proposed by Pike and collaborators [1]. The motivation of using FORC diagrams in the magnetic characterization of various magnetic materials is due to straightforwardness of the experimental method, because for any magnetic systems the FORCs can be easily measured and the FORC diagram can be calculated. The link between the FORC diagram and the Preisach distribution has been discussed in [2]. When applied to soft magnetic materials, FORC diagram is a sensitive tool that can probe subtle changes in hysteresis behavior and can provide understanding of various specific mechanism as the Domain Wall (DW) pinning, DW interactions, DW nucleation and annihilation, and DW curvature.

In this paper we have used Jiles-Atherton model to simulate the first order reversal curves and also we calculate the FORC diagrams in different conditions.

2. FORC curves and Jiles-Atherton model

The Jiles-Atherton model is one of the common model for description of the magnetization process in soft magnetic materials [3]. The magnetic susceptibility in Jiles-Atherton model is described by the differential equation:

$$\frac{dM}{dH} = \frac{(1-c)(M_{an}-M)}{\delta k(1-c)-\alpha(M_{an}-M)} + c\frac{dM_{an}}{dH} \tag{1}$$

where k is the pinning parameter, α is the mean field parameter c describe the shape of the anhysteretic curve, M_{an} is the anhysteretic magnetization and δ is a constant that equals +1 for ascendant hysteresis curve and -1 for descendant hysteresis curve.

* Corresponding author: mfecioru@stoner.phys.uaic.ro

We have simulated the FORC curves with Jiles-Atherton model, and we observed the presence of regions with negative susceptibility, at proximity of the reversal fields (see Fig 1).

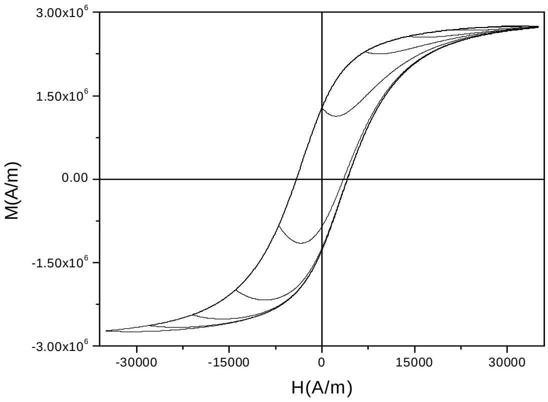

Fig. 1. FORC curves obtained on base of Jiles-Atherton model.

Because of the presence of these regions with negative susceptibility, we have used the Jiles-Atherton model in Jonathan-Deane version, [4], in which the magnetic susceptibility is described by the differential equation (2).

$$\frac{dM}{dH} = \delta_0 \cdot \frac{(1-c)(M_{an}-M)}{\delta k(1-c)-\alpha(M_{an}-M)} + c\frac{dM_{an}}{dH} \tag{2}$$

where,

$$\delta_0 = \begin{cases} 0, if .H < 0 \cdot and \cdot M_{an}(H_e) - M(H) \geq 0 \\ 0, if \cdot H \geq 0 \cdot and \cdot M_{an}(H_e) - M(H) \leq 0 \\ 1, otherwise \end{cases} \tag{3}$$

The FORC curves which were obtained in this case are present in Fig. 2-a. We observe that the regions with negative susceptibility do not appear, in this case.

We have simulated systematically FORC curves with Jiles-Atherton model, in Jonathn-Deane variant, and we calculated the FORC diagrams. In Fig. 2-b we present the FORC diagram which was obtained on the basis of this model, and in which the pinning parameter of the model (k), is independent on the applied magnetic field.

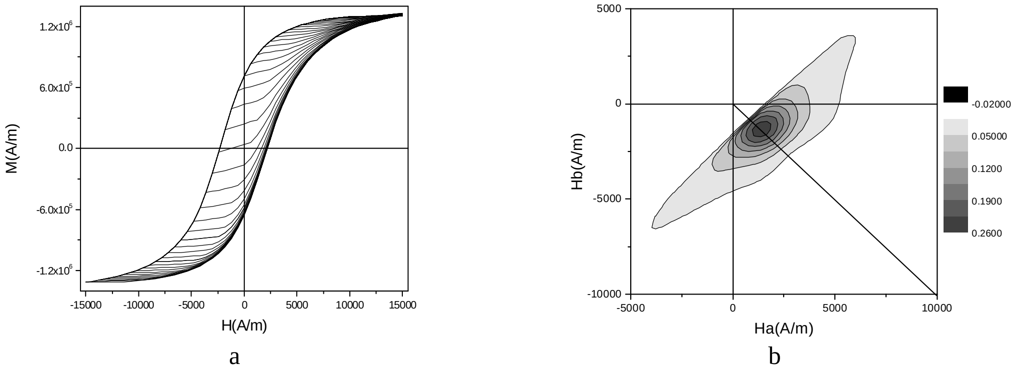

Fig. 2. (a) FORC curves obtained using Eq. (2); (b) FORC diagram obtained on the basis of Jiles – Atherton in Jonathan – Deane variant. The model parameters: $M_s = 1.5\times10^6$ A/m, a = 1600 A/m, $\alpha = 0.002$, c = 0.13, k = 1400 A/m.

In this case, we observe that the FORC distribution, which was obtained for a constant value of the pinning parameter for all values of applied magnetic field, do not have big values in direction of coercivity field axis like in experimental FORC diagrams from [5]. Therefore, we have decided to adapt the Jiles-Atherton model for a correct description of FORC diagrams for soft magnetic materials.

3. The pinning parameter depends on the applied magnetic field

The magnetization process in soft magnetic materials to be due reversible and irreversible changes of places of the domain wall and rotations of spontaneous magnetization of the magnetic domain. At small values of the applied magnetic field, the predominant mechanism of magnetization process is the displacement of domain wall. The pinning parameter is a measure of non-homogeneity of the soft magnetic material, which constitutes the pinning place for domain wall, and then, the values of pinning parameter will be high at small values of applied magnetic field and will be low at significantly large value of the applied magnetic field.

Therefore, we have considered the shape of pinning parameters as a Gaussian function of applied magnetic field:

$$k = k_0 \exp\left(-\frac{H_a - H_{a0}}{\sigma_a}\right)^2, \tag{4}$$

where H_a, is the applied magnetic field, H_{a0} is the value of the applied magnetic field corresponding to the maximum value of the pinning parameters and σ_a is the scattering of H_a values. In this case, we have plotted the first order reversal curves and we present in Fig. 3 the FORC diagram obtained.

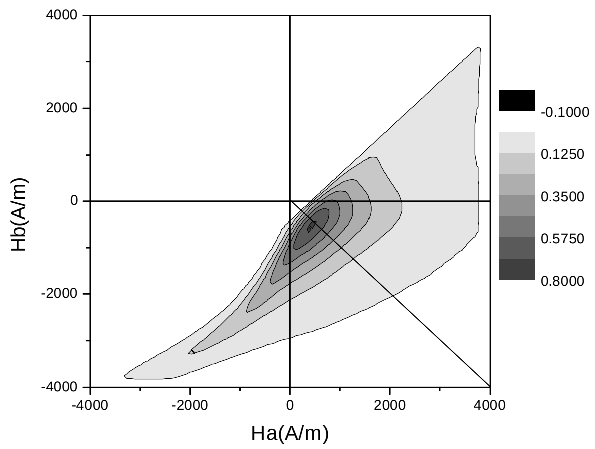

Fig. 3. FORC diagram obtained with Gaussian shape of pinning parameter. The model parameters: Ms =1.5×10^6A/m, a = 350 A/m, α = 1e-4, c = 0.33, H_{a0} = 500 A/m, k_0 = 700 A/m.

From Fig. 3 one observes that the FORC distribution, obtained with a Gaussian shape for pinning parameter, develops in the H_a direction, indicating an increase of values of FORC distribution in applied magnetic field direction and also, indicating an increase of average coercivity values. Therefore, in this case, we don't have large values of FORC distribution in the direction of coercivity field axis like in the experimental FORC diagrams [5]. Therefore, we have used a shape for the pinning parameter which depends on the applied magnetic field and on the reversal field. We have considered the shape of pinning parameters as a sum of two terms (Eq. (5)): the first term is independent of applied magnetic field and the second term is a Gaussian function on the coercivity field.

$$k = k_0 + k_1 \exp\left(-\frac{(H_a - H_b)/2}{\sigma_c}\right) , \tag{5}$$

where H_a is the applied magnetic field, H_b is the reversal field, and σ_c is the scattering of H_c values. Also, we have plotted the FORC curves with this shape for pinning parameter and we present in Fig. 4b the FORC diagram obtained.

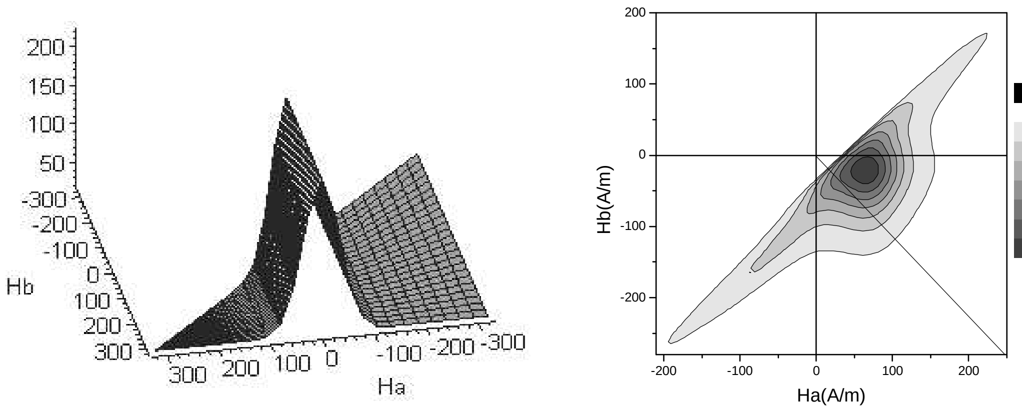

a b

Fig. 4. (a) - Shape of pinning parameter which depend of applied magnetic field and the reversal field; (b) - FORC diagram obtained with pinning parameter like in Eq (5). The model parameters: Ms = 79000 A/m, a =20 A/m, c = 0.1, $\alpha = 1 \times 10^{-4}$, k_0 = 20 A/m, σ_c = 40, k_1 = 80 A/m.

In Fig.4-b we can observe that the FORC distribution develops in the coercivity field H_c direction, indicating an increase of values of FORC distribution in the direction of coercivity field. This FORC diagram appears, approximately, like experimental FORC diagrams for soft magnetic materials.

In addition, we have considered a particular shape for the pinning parameter, in which k is composed of two terms: the first term (k_0) is independent of the applied magnetic field, and the second term has been obtained by multiplication between two terms: one term is a Gaussian function by the magnetic field and the other term has the particular shape, like in Eq. (6). H_a is the applied magnetic field, H_b is the reversal field, σ_c is the scattering of H_c values, and σ_a is the scattering of H_a values.

$$k = k_0 + k_1 \exp\left(-\frac{\ln\left(\frac{H_a - H_b}{2}\right)^2}{\sigma_c \frac{H_a - H_b}{2}}\right) \exp\left(-\frac{\left(\frac{H_a - H_{a0}}{2}\right)^2}{\sigma_a}\right) \tag{6}$$

We have plotted the FORC curves with this particular shape for pinning parameter and we have simulated the FORC diagrams. We present in Fig. 5-b the FORC diagrams obtained in this case.

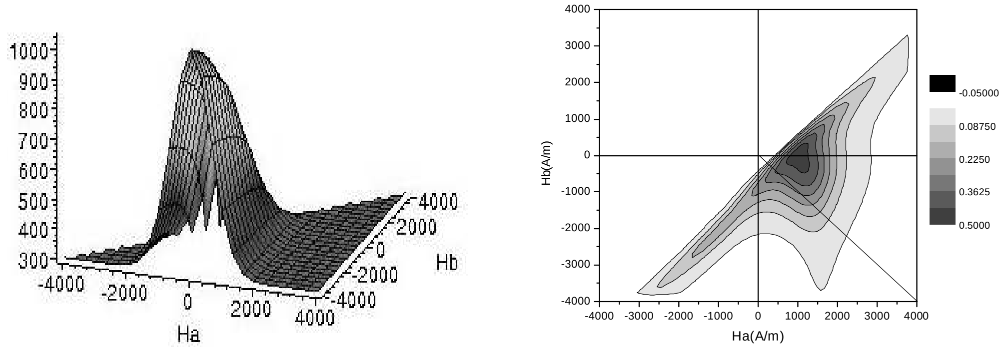

a b

Fig. 5. (a) - Shape of pinning parameter describes by Eq. (6); (b) - FORC diagram obtained. The model parameters: Ms = 1.5×10^6 A/m, a = 500 A/m, c = 0.2, $\alpha = 10^{-4}$, k_0 = 300 A/m, k_1 = 2000 A/m.

From Fig. 5-b we can observe that the FORC distribution develops in the coercivity field H_c direction. This FORC diagram is in concordance with experimental FORC diagrams for soft magnetic materials [1],[5]. This involve that for we obtained the FORC diagrams in concordance with experimental FORC diagrams on the basis of the Jiles-Atherton model, the shape of pinning parameter must be find according to Eq. (6) and it must be dependent on the applied field and the reversal field.

4. Depndence of FORC diagrams on Jiles-Atherton model parameters

Jiles-Atherton model is a phenomenological model for describing the magnetization curves for soft magnetic materials, and its parameters are known. We have used the shape for pinning parameter given by Eq. (6) and we have studied the dependence of FORC diagram as a function of the values of the new pinning parameter (k_1) and as o function of the values of the mean field parameter (α).We present in Fig. 6 the simulated FORC diagrams for three different values of pinning parameter k_1 but for the same values of otherwise parameters. One can observe that the FORC distribution develops in the H_c direction when the pinning parameter k_1 increases, indicating an increase of the values of FORC distribution in direction of coercivity field.

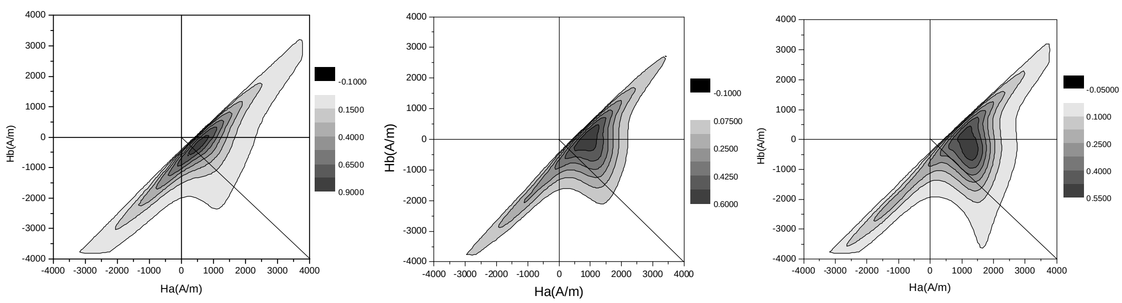

a b c

Fig. 6. FORC diagrams with different value for pinning parameters. The model parameters: Ms = 1.5×10^6 A/m, a = 500 A/m, c = 0.2, $\alpha = 10^{-4}$, k_0 = 300 A/m, (a) - k1 = 500 A/m, (b) - k1= 1800 A/m, (c) - k1= 3000 A/m.

This means that the values of FORC distribution increase when the average density of pinning site increases.

Also, we have studied the dependence of FORC diagrams as a function of the values of the mean field parameter, for the same values of the other parameters, and we present in Fig. 7 the simulated FORC diagrams for three different values of mean field parameter. We can observe a reduction of significant values of FORC distributions along the interactions field axis when the mean field parameter values are increasing.

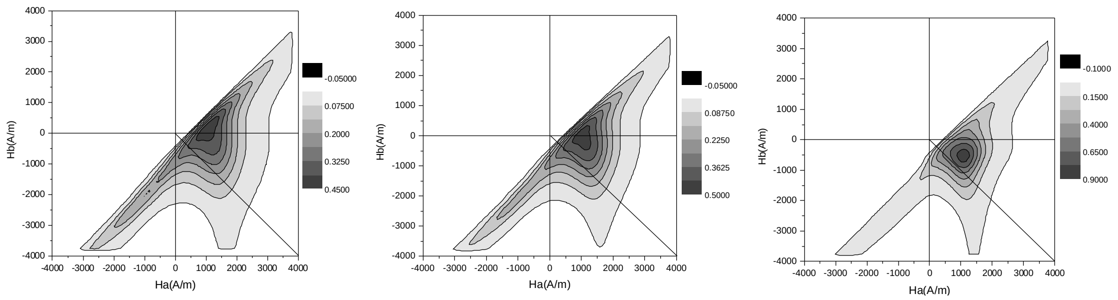

a b c

Fig. 7. FORC diagrams with different value for mean field parameter. The model parameters: Ms = 1.5×10^6 A/m, a = 500 A/m, c = 0.2, k_0 = 300 A/m, k_1 = 2000 A/m, (a) - $\alpha = 10^{-7}$, (b) - $\alpha = 10^{-4}$, (c) - $\alpha = 4\times10^{-4}$.

5. Conclusions

In this study we have used the Jiles-Atherton model in order to calculate the FORC diagrams for soft magnetic materials and we have shown that the pinning parameter of Jiles-Atherton model is dependent on the applied magnetic field and the reversal field. Also, we have shown that the FORC diagrams depend on the Jiles-Atherton model parameters and we studied this dependence. When the pinning parameter k_1 is increasing the FORC distribution develops in the H_c direction, indicating an increase of the values of FORC distribution in direction of coercivity field. Also, when the mean field parameter values are increasing we observe a reduction of significant values of FORC distributions along the interaction field axis.

References

[1] C. R. Pike, A. P. Roberts, K. L. Verosub, J. Appl. Phys. **85**(9), 6660 (1999).
[2] A. Stancu, C. R. Pike, L. Stoleriu, P. Postolache, D. Cimpoesu, J. Appl. Phys. **93**(10), 6620 (2003).
[3] D. C. Jiles, D. L. Atherton, J. Appl. Phys. **55**(6), 2115 (1984).
[4] H. Jonathan, B. Deane, IEEE Trans. on Magn. **30**(5), 2795 (1994).
[5] C. R. Pike, A. P. Roberts, M. J. Jekkers, K. L. Verosub, Phys. of the Earth and Planetary Interiors **126**, 11 (2001).